

## **Proton loading of jets and other consequences of the injection of neutrons in accretion flows**

Gabriela S. Vila,<sup>1</sup> Florencia L. Vieyro,<sup>1</sup> and Gustavo E. Romero<sup>1,2</sup>

<sup>1</sup>*Instituto Argentino de Radioastronomía, C.C. 5, (1894) Villa Elisa, Buenos Aires, Argentina*

<sup>2</sup>*Facultad de Cs. Astronómicas y Geofísicas, Universidad Nacional de La Plata, Paseo del Bosque S/N, (1900) La Plata, Buenos Aires, Argentina*

**Abstract.** Relativistic neutrons are injected in the corona surrounding an accreting black hole through hadronic interactions of locally accelerated protons. If the source is a microquasar, a fraction of these neutrons may escape and penetrate the base of the jet. The neutrons will decay into protons inside the outflow, this being then a possible mechanism for loading Poynting-dominated jets with baryons. We study the characteristics of the proton distribution injected in this way and the consequences on the high-energy radiative spectrum of the jet. We also investigate the fate of those neutrons that escape the corona into the external medium.

### **1. Introduction**

The composition of relativistic jets is an open issue. All relativistic jets emit synchrotron radiation at radio wavelengths. The characteristics of the radio spectrum give very strong evidence in favour of the presence of accelerated electrons (or electron-positron pairs) with a non-thermal distribution. The radiative output from protons may be largely unimportant unless they are accelerated to very high energies and find suitable targets to interact, such as a dense matter field or an intense magnetic field.<sup>1</sup> Currently, observational evidence of a baryonic component exists only for two accreting black holes: the galactic microquasars SS 433 and 4U1630-47 (Migliari et al. 2002, Díaz Trigo et al. 2013). The X-ray spectra of these objects show blueshifted iron lines. The inferred velocity of the iron nuclei ( $\sim 0.3 - 0.4c$ ) is consistent with the interpretation that they are traveling with the jets.

The question of composition is relevant because it is expected to be related to the launching mechanism of the outflows. Jets launched through the Blandford-Znajek process (e.g. Blandford & Znajek 1977) or similar (i.e. powered by the rotational energy of the black hole) are basically a Poynting flux plus electron-positron pairs created in situ. If, on the other hand, the outflows are launched and fed with matter from the accretion disk as a collimated wind (e.g. Blandford & Payne 1982), they should contain as well protons and other nuclei.

The launching mechanism, however, is definitively not the only factor that determines the composition of jets. Black hole-driven jets may get loaded with baryons by

---

<sup>1</sup>See for example Romero et al. (2003) and Vila et al. (2012) for models of hadronic emission of jets in microquasars.

entrainment with the matter in the medium they traverse – the outflows from the outer accretion disk or the wind of a companion star in a high-mass microquasar, for example.

In low-luminosity active galactic nuclei (AGN) and X-ray binaries (XRBs), observations support the existence of an advection-dominated and radiatively inefficient hot cloud of plasma around the compact object. This “corona” is usually modeled as a two-temperature ion-electron thermal plasma, sometimes with the addition of a population of non-thermal electrons or electron-positron pairs, see e.g. Vurm & Poutanen (2009). Compton up-scattering of disk photons by the electrons in the corona is the classical explanation for the origin of the power-law hard X-ray spectrum observed during the low-hard state of XRBs.<sup>2</sup> Recently, Romero et al. (2010), Vieyro et al. (2012) and Vieyro & Romero (2012) developed a radiative model for magnetized coronae in black hole XRBs that includes relativistic protons. They applied the model to Cygnus X-1, successfully reproducing the MeV emission detected by COMPTEL and *INTEGRAL* (McConnell et al. 2000, Cadolle Bell et al. 2006, Jourdain et al. 2012).

Relativistic protons in the corona produce gamma rays through the decay of neutral pions created in inelastic collisions with thermal protons. In about a half of the  $pp$  collisions the proton turns into a neutron. The conditions in the corona are such that the neutrons escape virtually without interacting and propagate for long distances until they decay. A fraction of these neutrons will enter the jets (if they exist) and decay there, injecting a proton and an electron that will get trapped by the local magnetic field and advected with the outflows. This is, then, another possible mechanism to load jets with protons.

The production and escape of neutrons from the central regions in AGN has been studied before by several authors, see e.g. Sikora et al. (1989), Bednarek (1992), Atoyan & Dermer (2003), and Toma & Takahara (2012). Here, we study the injection of neutrons in the magnetized corona of a microquasar through interactions of non-thermal protons with matter and radiation. We show that the neutrons escape the corona almost freely, and calculate their distribution in energy and space outside the source. We also compute the local spectrum of the protons and electrons injected where the neutrons decay. For those protons injected inside the jets, we estimate their high-energy emission by the interaction with a dense clump in the wind of the companion star. Finally, we discuss the characteristics of the radiation from the electrons injected far from the corona.

## 2. Corona model

We apply the corona model developed by Romero et al. (2010), Vieyro et al. (2012) and Vieyro & Romero (2012). The reader is referred to those works for a detailed description of the model, here we only comment briefly on its most important aspects.

We assume the corona to be homogeneous and spherical, with a radius of  $R_c = 35R_{\text{grav}}$  (the mass of the black hole is  $15M_\odot$ , as in Cygnus X-1). The bolometric luminosity of the corona is  $L_c = 0.01L_{\text{Edd}} \approx 10^{37} \text{ erg s}^{-1}$ . The mean number density of thermal protons and electrons in the corona is  $n_{p,e} \approx 10^{13} \text{ cm}^{-3}$ . The hypothesis of

---

<sup>2</sup>This emission may as well be synchrotron radiation from electrons in the jets, see Vila & Romero (2009) and Vila et al. (2012).

equipartition between the energy density of thermal particles and the magnetic energy density, yields a mean magnetic field strength  $B_c \approx 10^5$  G.

Relativistic protons are injected in the corona with a power-law energy spectrum  $Q_p \propto E_p^{-2.2}$  [ $\text{erg}^{-1} \text{cm}^{-3}$ ]. This is consistent with a diffusive acceleration mechanism, that in the corona may operate at sites of fast magnetic reconnection (de Gouveia dal Pino & Lazarian 2005, but see also Drury 2012). The steady-state distribution of relativistic protons  $N_p(E_p)$  [ $\text{erg}^{-1} \text{cm}^{-3}$ ] is calculated solving a system of kinetic equations that couple the behaviour of protons, electrons, and photons in the corona. The equation for each particle species includes terms that account for injection, energy losses, and escape.

The relativistic protons in the corona cool as they interact with the thermal protons, the non-thermal radiation emitted by the relativistic electrons, the blackbody photons from the accretion disk, and the Comptonized disk photons. The latter is the most relevant radiation field, that we parametrize as a power-law with a cutoff of the form  $n_{\text{ph}} \propto E_{\text{ph}}^{-\beta} \exp(-E_{\text{ph}}/E_0)$  with  $\beta = 1.6$  and  $E_0 = 150$  keV.

The main channels of proton-proton ( $pp$ ) and proton-photon ( $p\gamma$ ) collisions that produce neutrons are

$$\begin{aligned} p + p &\rightarrow p + n + \pi^+ + a\pi^0 + b(\pi^+ + \pi), \\ p + p &\rightarrow n + n + 2\pi^+ + a\pi^0 + b(\pi^+ + \pi), \\ p + \gamma &\rightarrow n + \pi^+ + a\pi^0 + b(\pi^+ + \pi), \end{aligned} \quad (1)$$

where the integers  $a, b$  are the pion multiplicities. To calculate the neutron injection functions we adopt the parameterizations given by Sikora (1989), Atoyan (1992), and Atoyan & Dermer (2003).

### 3. Results

The left panel of Figure 1 shows the injection rates of neutrons created in  $pp$  and  $p\gamma$  interactions, as a function of energy. The total power injected in neutrons inside the corona is  $L_n \approx 6 \times 10^{35} \text{ erg s}^{-1}$ . The cooling rates for neutrons by collisions with protons and photons, the decay rate, and the inverse of the corona crossing time are plotted in the right panel of Figure 1. The escape time is the shortest for all energies considered, so we make the approximation that all neutrons leave the corona before decaying without losing energy.

The steady-state distribution of neutrons in energy and space outside the corona, may be written as  $N_n(E_n, r) \propto r^{-2} \exp(-r/r_\tau)$ , where  $\tau(E_n)$  and  $v_n(E_n)$  are the mean lifetime and the velocity of the neutrons, respectively, and  $r_\tau = \tau_n v_n$ . The coordinate  $r$  is the radial distance to the center of the corona. Each neutron injects a proton, an electron, and an electron antineutrino at decay,  $n \rightarrow p + e^- + \bar{\nu}_e$ . The proton carries  $\sim 99.9\%$  of the energy of the neutron, so the proton injection function is well approximated as  $Q_p^{n \rightarrow p}(E_p, r) \approx N_n(E_n, r)/\tau(E_n)$  with  $E_p = 0.999E_n$ . To calculate the injection rate of electrons we followed Abraham et al. (1966). The results are shown in Figure 2. The total power injected in protons is  $\sim 10^{35} \text{ erg s}^{-1}$  whereas the power in electrons is  $\sim 10^{30} \text{ erg s}^{-1}$ . Most of these particles are created within  $r \approx 10^{12-13} \text{ cm}$ , a region whose size is of the order of the size of the binary system.

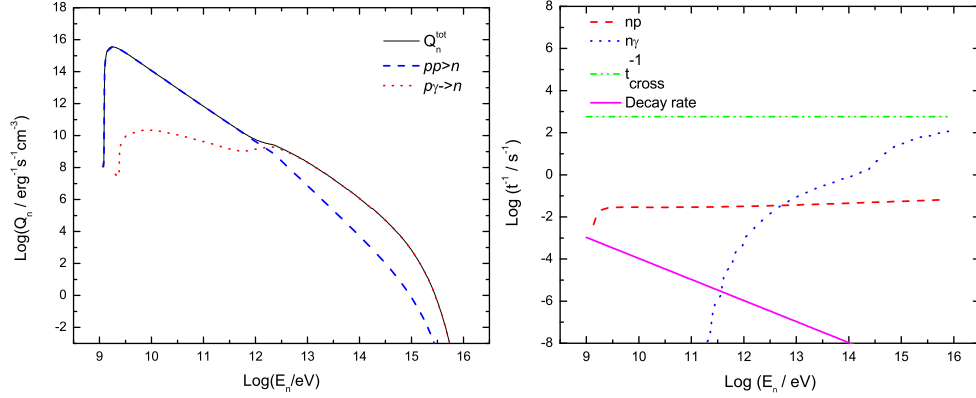


Figure 1. Left: injection rate of neutrons as a function on energy inside. Right: cooling, escape, and decay rates of neutrons in the corona.

To estimate the fraction of neutrons that decay inside the jets, we assumed that these are launched at a distance  $50R_{\text{grav}}$  from the black hole, and that they are conical with a half opening angle  $\sim 6^\circ$ . For this choice of geometry, the decay of neutrons along the jets (up to  $r \sim 10^{12}$  cm) injects a total power  $\sim 10^{34}$  erg s $^{-1}$  in protons. Notice that these protons are non-thermal: their energy distribution mimics that of the parent neutrons, that in turn depends on that of the relativistic protons in the corona.

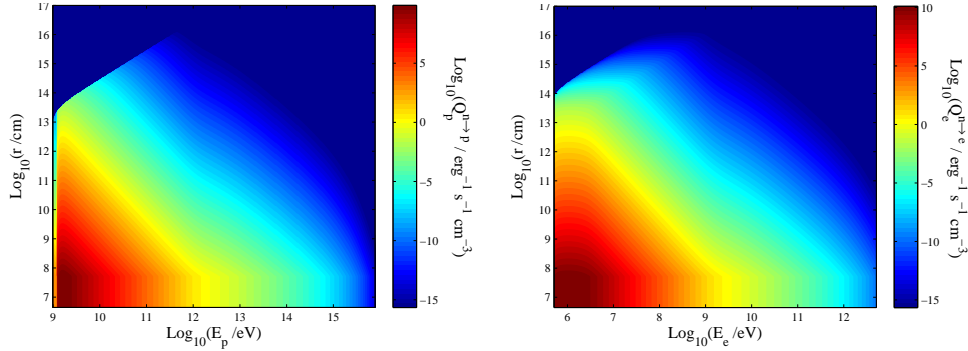


Figure 2. Left: injection spectrum of protons by decay of neutrons as a function of energy and distance to the black hole. Right: the same but for electrons.

If the companion star is a massive, young star with strong winds, the clumps in the wind may penetrate the jet. These clumps are dense and therefore suitable targets for the relativistic protons in the jets, producing gamma rays by decay of neutral pions decays from  $pp$  collisions (Araudo et al. 2009). Applying the model of Romero & Vila (2008) and Vila et al. (2012) to characterize the jets, we estimate the gamma-ray spectrum for different combinations of size, density, and location of the clump. The results are shown in Fig. 3.

Much less power is injected in electrons than in protons. Electrons, however, cool very efficiently. Those injected within the binary system will interact with the magnetic field and the radiation field of the companion star. For a massive star, typical values

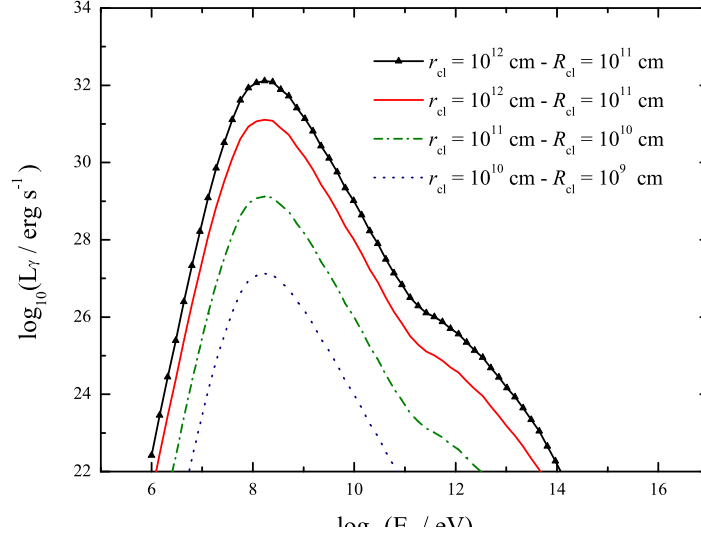


Figure 3. Gamma-ray emission from  $pp$  collisions in a jet-clump interaction, for different values of the clump radius  $R_{\text{cl}}$  and distance to the black hole  $r_{\text{cl}}$ . The density of the clump is  $n_{\text{cl}} = 10^{12} \text{ cm}^{-3}$ , except for the black symbol-line curve where  $n_{\text{cl}} = 10^{13} \text{ cm}^{-3}$ .

of magnetic field and temperature at the surface are  $B_{\star} \sim 100 \text{ G}$  and  $T_{\star} \sim 10^4 \text{ K}$ . Under these conditions the cooling times of electrons are very long, so they will diffuse far from their injection site before losing an appreciable fraction of their energy. The calculation of the radiative spectrum of the electrons and of the morphology of the emission region must be carried out accounting for propagation effects as in Bosch-Ramon & Khangulyan (2011). For the electron energies and magnetic fields considered here, the formation of a radio synchrotron nebula at  $\sim \text{GHz}$  frequencies may be expected. If electrons cool predominantly through this channel, the nebula should be detectable at the level of the mJy at 1 GHz for a source at  $\sim 2 \text{ kpc}$ .

#### 4. Summary and perspectives

We have studied the production of neutrons in the corona of an accreting stellar-mass black hole. The decay of these neutrons inside the jets - if present - is a way of loading them with baryons irrespective of the launching mechanism. These protons are energetic and have a non-thermal distribution; they may produce gamma rays by interaction with a dense matter target such as a clump from the wind of the companion star. Although according to our results the power in protons is low, the added contribution of several quasi-simultaneous jet-clump interactions may give rise to weak flaring emission at GeV energies, such as that recently observed in Cygnus X-1 by Bodaghee et al. (2013). The cooling of electrons injected outside the corona should create a detectable radio nebula at scales of the size of the binary system. The detailed structure of the nebula will be addressed elsewhere.

**Acknowledgments.** This research was supported by grants PIP 0078/2010 and PICT 2012-00878 Préstamo BID.

**References**

- Abraham, P. B., Brunstein, K. A. & Cline, T. L. 1966, *Phys. Rev.*, 150, 1088
- Araudo, A. T., Bosch-Ramon, V. & Romero, G. E. 2009, *A&A*, 503, 673
- Atoyan, A. 1992, *A&A*, 257, 465
- Bednarek, W. 1992, *A&A*, 264, 331
- Blandford, R. D. & Payne, D. G. 1982, *MNRAS*, 199, 883
- Blandford, R. D. & Znajek, R. L. 1977, *MNRAS*, 179, 433
- Bodaghee, A. et al. 2013, *ApJ*, 775, id.98
- Cadolle Bel, M. et al. 2006, *A&A*, 446, 591
- de Gouveia dal Pino, E. M. & Lazarian, A. 2005, *A&A*, 441, 845
- Díaz-Trigo, R., Miller-Jones, J. C. A., Migliari, S. et al. 2013, *Nature*, 504, 260
- Drury, L. O'C. 2012, *MNRAS*, 422, 2474
- Jourdain, E., Roques, J. P. & Malzac, J. 2012, *ApJ*, 744, id.64
- McConnell, M. L. et al. 2000, *ApJ*, 543, 928
- Migliari, S., Fender, R. & Méndez, M. 2002, *Science*, 297, 1673
- Romero, G. E., Vieyro, F. L. & Vila, G. S. 2010, *A&A*, 519, id.A109
- Romero, G. E. & Vila, G. S. 2008, *A&A*, 485, 623
- Romero, G. E. et al. 2003, *A&A*, 410, L1
- Sikora, M., Begelman, M. & Rudak, B. 1989, *ApJ*, 341, L33
- Toma, K. & Takahara, F. 2012, *ApJ*, 754, 148
- Vieyro, F. L. & Romero, G. E. 2012, *A&A*, 542, id.A7
- Vieyro, F. L. et al. 2012, *A&A*, 546, id.A46
- Vila, G. S. & Romero, G. E. 2010, *MNRAS*, 403, 1457
- Vila, G. S., Romero, G. E. & Casco, N. A. 2012, *A&A*, 538, id.A97
- Vurm, I. & Poutanen, J. 2009, *ApJ*, 698, 29